Activation of Adenosine Monophosphate—Activated Protein Kinase Reduces the Onset of Diet-Induced Hepatocellular Carcinoma in Mice

Dieter Schmoll,[1] Nicole Ziegler,[1] Benoit Viollet,[2] Marc Foretz,[2] Patrick C. Even,[3] Dalila Azzout-Marniche,[3] Andreas Nygaard Madsen,[4] Martin Illemann,[4] Karen Mandrup (iD) ,[4] Michael Feigh,[4] Jörg Czech,[1] Heiner Glombik,[1] Jacob A. Olsen,[1] Wolfgang Hennerici,[1] Klaus Steinmeyer,[1] Ralf Elvert,[1] Tamara R. Castañeda,[1] and Aimo Kannt[1,5,6]

The worldwide obesity and type 2 diabetes epidemics have led to an increase in nonalcoholic fatty liver disease (NAFLD). NAFLD covers a spectrum of hepatic pathologies ranging from simple steatosis to nonalcoholic steatohepatitis, characterized by fibrosis and hepatic inflammation. Nonalcoholic steatohepatitis predisposes to the onset of hepatocellular carcinoma (HCC). Here, we characterized the effect of a pharmacological activator of the intracellular energy sensor adenosine monophosphate–activated protein kinase (AMPK) on NAFLD progression in a mouse model. The compound stimulated fat oxidation by activating AMPK in both liver and skeletal muscle, as revealed by indirect calorimetry. This translated into an ameliorated hepatic steatosis and reduced fibrosis progression in mice fed a diet high in fat, cholesterol, and fructose for 20 weeks. Feeding mice this diet for 80 weeks caused the onset of HCC. The administration of the AMPK activator for 12 weeks significantly reduced tumor incidence and size. *Conclusion:* Pharmacological activation of AMPK reduces NAFLD progression to HCC in preclinical models. (*Hepatology Communications* 2020;4:1056-1072).

Nonalcoholic fatty liver disease (NAFLD) is a chronic liver disease with increasing incidence driven by the pandemic spread of obesity and type 2 diabetes. NAFLD starts as simple steatosis and can develop into nonalcoholic steatohepatitis (NASH) with its hallmarks of steatosis, inflammation, and liver injury. NASH predisposes to the onset of liver cirrhosis and hepatocellular carcinoma (HCC).[1,2] NAFLD is the fastest-growing cause of HCC.[1,2] The molecular pathogenesis of NAFLD is not completely understood but is most likely multifactorial. It is favored by genetics as well as features of the metabolic syndrome,

such as obesity and hepatic insulin resistance. On the molecular level, the participation of oxidative stress, lipotoxicity, proinflammatory cytokines, infiltrated immune cells, and alterations in the gut microbiome has been postulated.[1,3] There is currently no effective treatment available to prevent the progression of NASH to HCC.

Adenosine monophosphate–activated protein kinase (AMPK) is stimulated in response to an increased AMP/adenosine triphosphate (ATP) ratio, which enables the enzyme to act as an intracellular energy sensor. The subsequent phosphorylation of several protein targets activates downstream catabolic pathways, to restore cellular energy charge.[4,5] The enzyme is a heterotrimer consisting of α, β, and γ subunits. Each subunit is encoded by multiple genes, leading to the expression of 12 AMPK isoforms in a tissue-selective manner.[4] In recent years, highly selective pharmacological AMPK activators have been identified and studied for the treatment of several diseases.[4,6-9] Small-molecule activators that activate β2-containing AMPK isoforms expressed in muscle have an antidiabetic effect, predominantly by the stimulation of glucose uptake.[6,8] Both the pharmacological and genetic activation of hepatic AMPK improve steatosis, suggesting that AMPK activation could also be a useful strategy for the treatment of early stages of NAFLD.[7,10-13]

In the present study, we characterized a compound that activates AMPK in both liver and muscle. This compound improves both hepatic steatosis and fibrosis, and reduces the onset of HCC in a rodent model of NASH.

Materials and Methods

SYNTHESIS

Compound 1 was synthesized as described[14] and is outlined briefly in Supporting Fig. S1.

IN VITRO ASSAY

Recombinant AMPK isoforms were obtained from SignalChem (Richmond, BC, Canada). AMPK activity was measured using Caliper LabChip technology (PerkinElmer, Waltham, MA). The reaction mixture (9 μL) contained 100 mM 4-(2-hydroxyethyl)-1-piperazine ethanesulfonic acid (HEPES; pH 7.4), 10 mM $MgCl_2$, 1 mM dithiothreitol, 0.01% bovine serum albumin, 1 μM substrate peptide with the sequence H-HMRSAMSGLHLVK-Lys(FAM)-NH2, 50 μM ATP, compound 1 (0-33 μM), 1% dimethyl sulfoxide, and the respective AMPK isoforms (0.02 μg/mL). The reaction was stopped after 60 minutes by adding stop solution (100 mM HEPES, pH 7.4; 0.015% Triton X-100; and 20 mM ethylene diamine tetra-acetic acid [EDTA]). Fluorescence was measured using a Caliper EZReader2 (PerkinElmer). The EC150 value was defined as the compound concentration that stimulates the basal enzymatic activity by 50%. Phosphorylation of AMPK was measured in L6 cells (#CRL-1458; American Type Culture Collection, Manassas, VA) using an enzyme-linked immunosorbent assay (ELISA). Cells were incubated for 30 minutes with different concentrations of compound 1 and fixated with formaldehyde. After treatment with blocking reagent (Bio-Rad Laboratories,

ARTICLE INFORMATION:

From the [1]Sanofi R&D, Frankfurt, Germany; [2]Université de Paris, Institut Cochin, CNRS UMR 8104, INSERM U1016, Paris, France; [3]UMR Nutrition Physiology and Ingestive Behavior, AgroParisTech, INRA, Université Paris-Saclay, Paris, France; [4]Gubra, Hørsholm, Denmark; [5]Institute of Experimental Pharmacology, Medical Faculty Mannheim, University of Heidelberg, Mannheim, Germany; [6]Fraunhofer IME, Translational Medicine and Pharmacology, Frankfurt, Germany.

ADDRESS CORRESPONDENCE AND REPRINT REQUESTS TO:

Dieter Schmoll, Ph.D.
Sanofi R&D
Industriepark Höchst, H825

65926 Frankfurt, Germany
E-mail: Dieter.Schmoll@sanofi.com
Tel.: +49 069 305 16642

Hercules, CA), samples were incubated overnight with an anti-phosphorylated acetyl-coenzyme A carboxylase (ACC) antibody (#3661L; Cell Signaling Technology, Danvers, MA), washed, and subsequently treated with anti-rabbit horseradish peroxidase immunoglobulin (#7074S; Cell Signaling Technology). Chemiluminescence was detected using diphenylamine, 4-iodophenol, and H_2O_2 as substrates. Stimulation of fat oxidation was determined in L6 cells by measuring the release of ^3H_2O from [^3H]palmitate as described.[15]

SELECTIVITY ASSAYS

The interactions of 10 µM compound 1 with a panel of receptors, ion channels, enzymes, and protein kinases (Supporting Table S1) were tested by Eurofins Cerep (Celle-Lévescault, France).

ANIMAL STUDIES

All animals received humane care according to the criteria outlined in the *Guide for the Care and Use of Laboratory Animals* prepared by the National Academy of Sciences and published by the National Institutes of Health (publication 86-23, revised 1985).

PHARMACOKINETIC STUDIES

Pharmacokinetic (PK) studies of compound 1 were conducted in C57Bl/6 female mice using a composite study design with three animals per time point. A dose of 10 mg/kg was administered orally as a 1-mg/mL suspension of compound 1 in vehicle (0.6% methylcellulose in water), and a dose of 3 mg/kg was administered intravenously (IV) as a 1.2-mg/mL solution in 26% glycofurol/Cremophor (3:1) in water. Blood samples were collected in EDTA-containing tubes at 0.083 (only IV), 0.25, 0.5, 1, 2, 4, 6, 8, and 24 hours after compound administration and kept on ice until a minimum volume of 100 µL plasma was collected after centrifugation. Liquid chromatography–tandem mass spectrometry (LC-MS/MS) samples were prepared by dilution of plasma samples with 4 parts of water. To a 50-µL diluted plasma sample, a 150-µL solution of 0.1% formic acid in acetonitrile containing an internal standard (100 ng/mL) was added. Following centrifugation, 50 µL of supernatant was further diluted with 50 µL 0.1% formic acid in an acetonitrile–water ratio of 1:1. Compound 1 was then quantified with

LC-MS/MS from a standard curve. The LC-MS/MS system consisted of a Waters ACQUITY ultra-performance liquid chromatography (UPLC) system and a Waters Xevo triple quadrupole mass spectrometer (Milford, MA). Chromatographic separation was achieved on an ACQUITY UPLC Ethylene Bridged Hybrid C18 (1.7 µm 2.1 × 50 mm column at 40°C using a 0.8-mL/minute gradient of mobile phase A (0.1% formic acid in water) and mobile phase B (0.1% formic acid in acetonitrile): 0 minutes, 2% mobile phase B; 0.25 minutes, 2% mobile phase B; 1 minute, 98% mobile phase B; and 1.5 minutes, 98% mobile phase B. For compound 1, the retention time was 0.79 minutes, and the transition monitored was m/z 524.1 to 365.97. For the internal standard, the retention time was 0.98 minutes, and the transition monitored was m/z 474.1 to 160.89. Lower limit of quantification of compound 1 was 2.5 ng/mL. PK parameters were finally calculated by noncompartmental analysis using Phoenix WinNonlin software version 8.0.0.3176.

PHARMACOLOGICAL STUDIES IN KK-A^y MICE

Glucose tolerance was tested in 8-week-old and 9-week-old male lean KK/TaJcl and obese (ob/ob) KK-A^y/TaJcl mice (CLEA Japan, Inc., Shizuoka, Japan) fasted for 4.5 hours using a glucose bolus of 2 g/kg of body weight after acute oral administration of either compound 1 (2 and 10 mg/kg, 10 mL/kg) or vehicle (0.6% methylcellulose in water). Blood hemoglobin A1c (HbA1C) percent, serum ketone bodies, and liver triglycerides were determined after 3 weeks of single daily administration as described.[16,17]

AMYLIN LIVER NASH DIET−INDUCED NAFLD MODELS

The *ob/ob*-NASH model was carried out as described.[18,19] In brief, male *ob/ob* (Lep^ob/ob [C57BL/6J]) mice at 5 weeks of age were obtained from Janvier Labs (France) and fed either standard chow (Altromin 1324; Brogaarden, Denmark) or the amylin liver NASH (AMLN) diet containing 40% fat (18% trans fat), 40% carbohydrates (20% fructose), and 2% cholesterol (D09100301; Research Diets Inc., New Brunswick, NJ). After 12 weeks, a

liver biopsy was performed for histological assessment of individual fibrosis at baseline, and mice were kept single-housed. Mice were randomized into control or treatment groups based on body weight and liver fibrosis. Either compound 1 (5 mg/kg) or vehicle (0.6 % methylcellulose) was subsequently administered daily for 8 weeks per oral gavage. After a total of 20 weeks on AMLN diet, animals were euthanized, and liver tissue was collected for histological and biochemical analysis. A semiquantitative histological staging system was applied for scoring of hepatic steatosis (score 0-3), lobular inflammation (score 0-3), hepatocyte ballooning (score 0-2), and fibrosis (stage 0-4) using the criteria proposed by Kleiner et al.[20] The NAFLD activity score is the sum of steatosis, lobular inflammation, and hepatocellular ballooning scores.[20] Mice with fibrosis stage ≥ 1 were included in the study. The diet-induced HCC model was generated by feeding 5-week-old male C57BL/6J mice (Janvier Labs) either standard chow or the AMLN diet. After 63 weeks, liver biopsies were performed for the histological assessment of individual fibrosis. Subsequently, the mice were kept single-housed, and after 68 weeks on the respective diets, either compound 1 (3 mg/kg) or vehicle (0.6% methylcellulose and 0.5% Tween 80) was administered for 12 weeks. After a total of 80 weeks of AMLN diet, the animals were euthanized and their livers examined. Macroscopically visible tumors were measured (in millimeters), counted, and dissected from the livers for histological assessment. For histological examination, livers were fixed in formalin and embedded in paraffin. Sections of 3-μm thickness were cut, deparaffinated in xylene, and rehydrated in ethanol. Sections were stained with hematoxylin and eosin (HE) and picrosirius red (Sigma-Aldrich, Brondby, Denmark) and mounted with Pertex. For reticulin staining, slides were incubated with potassium permanganate solution, followed by sulfuric acid, oxalic acid, ferric ammonium sulfate solution, silver nitrate solution, formaldehyde solution, gold chloride solution, and sodium thiosulfate solution. Malignancy of liver tumors was assessed in HE-stained and reticulin-stained liver slides.

GENETIC MODELS

Indirect calorimetry and oral glucose tolerance tests were performed in male mice (C57BL/6J) without or with a loss of AMPK, either restricted to skeletal muscle or liver. The genetic models have been described.[10,21] All mice were kept in a barrier facility under a 12-hour light/12-hour dark cycle with free access to water and standard mouse diet (diet A03; SAFE, Augy, France) containing 65% carbohydrate, 11% fat, and 24% protein in terms of energy. Measurements of respiratory exchange ratio were performed in metabolic cages as described.[11] In brief, the metabolic cage was continuously connected to an open-circuit, indirect calorimetry system. Spontaneous activity was measured by means of three piezoelectric force transducers positioned in a triangular configuration under the metabolic cage. The electrical signals from the activity amplifier, flow meter, and O_2 and CO_2 analyzers were sampled at 100 Hz, averaged and stored every 2 seconds. Computer-assisted processing of respiratory exchanges and spontaneous activity signals was performed to extract the respiratory exchanges specifically associated with spontaneous activity (Kalman filtering method[22]). This separation provided information about total, resting, and activity-related O_2 consumption and CO_2 production. Airflow through the chamber was regulated at 0.5 L/minute by a mass flow meter, and temperature was maintained close to thermoneutrality (30°C ± 1°C). On the first day, mice were administered with vehicle, and oxygen consumption (VO_2) and carbon dioxide consumption (VCO_2) were recorded at 2-second intervals. On the following day, the mice were dosed with the compound, and VO_2 and VCO_2 recordings were continued for another 22 hours. The respiratory quotient (RQ) was calculated as the ratio of VCO_2 produced to VO_2 consumed; ΔRQ was calculated as change of RQ versus $t = 0$. Because the vehicle-treated animals showed no significant differences between the genotypes, they were grouped together. The metabolic rate (MR) was calculated using the formula MR (weight [W]) = $16.3 \times VO_2 + 4.57 \times VCO_2 \div 60$, as described.[22,23] The oral glucose tolerance test was performed as described previously in KK-A^y mice.

MESSENGER RNA ISOLATION AND QUANTITATIVE REAL-TIME POLYMERASE CHAIN REACTION

Quantitative real-time polymerase chain reaction (RT-PCR) was carried out as described[24] using the following primer sets (Applied Biosystems, Foster City, CA): ribosomal protein L37a (RPL37a; Mm

01546394_s1); ubiquitin D (UBD; Mm 01972246_s1); sidekick cell adhesion 1 (SDK1; Mm 00625905_m1); collagen type 1 alpha 1 (Col1a1; Mm 00801666_g1); and lipocalin 2 (LCN2) (Mm 01324470_m1).

IMMUNOBLOTTING

Immunoblots were carried out as described[24] using the following antibodies: AMPK (#2532; Cell Signaling Technology); Thr-172 phosphorylated AMPK (p-AMPK; #2535; Cell Signaling Technology); glyceraldehyde 3-phosphate dehydrogenase (#21118; Cell Signaling Technology); actin (#A2228, Sigma-Aldrich); and WNT1-inducible-signaling pathway protein 1 (Wisp1; #ab178547; Abcam, Cambridge, United Kingdom).

Results

Compound 1 (Fig. 1) activated 10 recombinant AMPK isoforms with high potency, including trimers containing the β2 subunit (Table 1). At a concentration of 10 μM, the compound did not significantly interact with a panel of 480 proteins, indicating high selectivity (Supporting Table S1). In L6 rat muscle cells, compound 1 induced the phosphorylation of ACC by 50% at a concentration of 0.45 ± 0.1 μM (Fig. 2A) and stimulated fat oxidation at a concentration of 1 μM to a similar extent, as was observed after omission of glucose in the culture medium (Fig. 2B). The PK profile of compound 1 in mice (Table 2) indicated an oral bioavailability of 85%. Up to 8 hours after dosing, the calculated free plasma levels of compound 1 at an oral

FIG. 1. Structure of compound 1.

TABLE 1. *IN VITRO* ACTIVITY OF COMPOUND 1

AMPK Isoform	EC150 (nM)
α1β1γ1	0.337
α1β1γ3	0.398
α2β1γ1	0.376
α2β1γ2	0.252
α1β2γ1	0.384
α1β2γ2	0.876
α1β2γ3	0.95
α2β2γ1	0.221
α2β2γ2	0.196
α2β2γ3	0.404

Note: EC150 value was defined as the compound concentration that stimulates the basal enzymatic activity by 50%.

dose of 10 mg/kg were considerably higher than the EC150 values in the *in vitro* assays (Fig. 3), indicating the potential for once-daily dosing.

We established the pharmacologically active dose range of compound 1 in obese KK-A^y mice. Single administration of compound 1 at doses of 2 and 10 mg/kg improved oral glucose tolerance (Fig. 4). The daily administration of either dose over 3 weeks reduced blood HbA1c and hepatic triglycerides. Plasma ketone body levels were increased, which suggests that the antisteatotic effect of compound 1 could be due to a stimulation of fat oxidation. To prove this, indirect calorimetry was performed. Compound 1 reduced ΔRQ (Fig. 5A) without affecting MR (Fig. 5B), demonstrating increased whole-body fat oxidation. Compound 1 activated AMPK both in liver and skeletal muscle, as demonstrated by the increased phosphorylation of the enzyme (Fig. 5C). To determine the relative contribution of AMPK activation in these tissues to the stimulation of whole-body fat oxidation, indirect calorimetry was performed in mice that had a loss of AMPK either in skeletal muscle or in liver. In both genetic models, the compound lowered the RQ (Fig. 5D,E). In relation to wild-type (WT) animals, the magnitude of this effect was attenuated in particular in mice lacking AMPK in skeletal muscle (Fig. 5F), in which the compound changed fuel selection by the stimulation of fat oxidation in both liver and skeletal muscle. In comparison, we performed an oral glucose tolerance test in both genotypes and WT mice. The loss of AMPK in liver did not change the improvement of glucose tolerance by the AMPK activator (Fig. 5G). However, in mice lacking AMPK in skeletal muscle, the compound effect
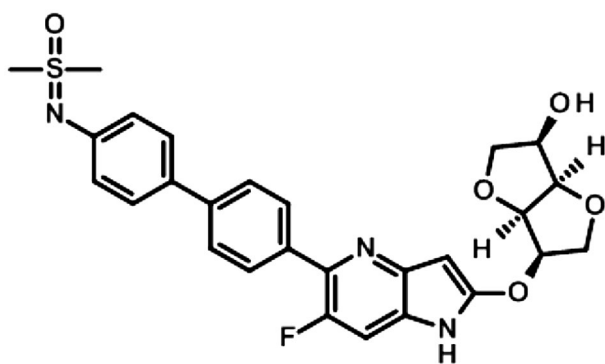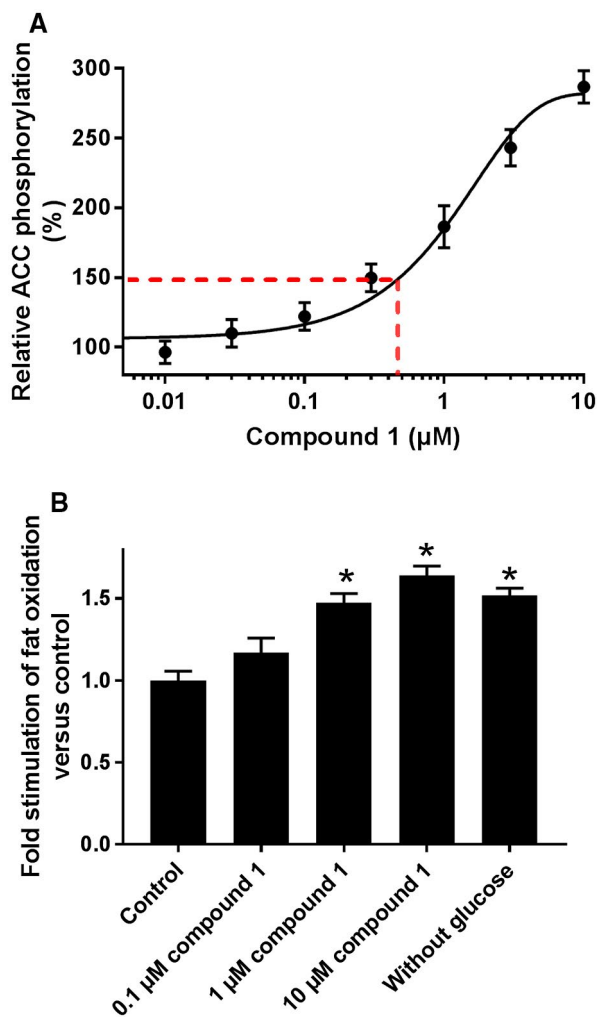
A

B

FIG. 2. Cellular activation of AMPK by compound 1. (A) Induction of ACC phosphorylation. L6 muscle cells were incubated in the absence or presence of compound 1 at the indicated concentrations. ACC phosphorylation was determined by ELISA. Data are expressed as the phosphorylation in relation to the chemiluminescence signal in the absence of compound 1, which was set as 100%. The EC150 value was defined as the compound concentration that increases the signal by 50%. Values are presented as means ± SEM (n = 3). (B) Stimulation of fat oxidation by compound 1. L6 muscle cells were incubated in the presence of [3H]palmitate and the indicated concentrations of compound 1. After 4 hours, the release of ^3H_2O was measured. Results are expressed as the fold induction of fat oxidation in relation to solvent control (0 μM compound 1). As a control for maximal fat oxidation, cells were also incubated in the absence of glucose. Values are presented as means ± SEM (n = 4); *$P < 0.05$ versus 0 μM compound 1.

was significantly attenuated (Fig. 5H). The data indicate that the compound improved glucose tolerance by the activation of AMPK in skeletal muscle but not in liver.

TABLE 2. PHARMACOKINETIC PARAMETERS OF COMPOUND 1

Administration	PK Parameter	
	10 mg/kg po	3 mg/kg IV
AUC (hours × ng/mL)	8,060	2,853
$T_{1/2}$ (hours)	2.1	3.1
Cmax (ng/mL)	1,555	—
Tmax (hours)	2.0	—
CLp (mL/min/kg)	—	18
Vdss (L/kg)	—	2.3
Bioavailability	85%	—

Note: Mice were administered compound 1 either 10 mg/kg po or 3 mg/kg IV.
Abbreviations: AUC, area under the curve; CLp, plasma clearance; Cmax, maximum concentration; po, per os administration; Tmax, time of maximum concentration; Vdss, volume of distribution.
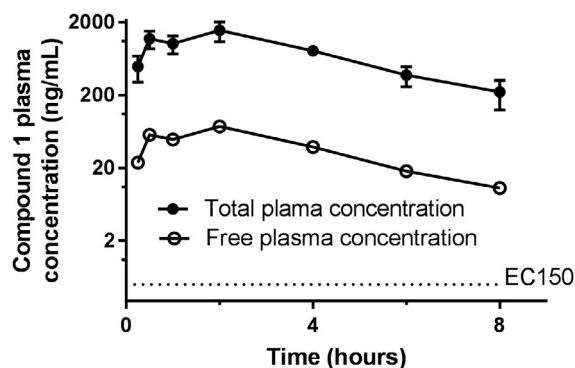

FIG. 3. Average plasma concentrations of compound 1 in C57Bl/6 female mice after a single oral dose of 10 mg/kg. Data are presented as means ± SD (n = 3). Average unbound plasma concentration of compound 1 was calculated from mouse plasma protein binding of compound 1. Dotted line represents the highest determined EC150 value of all the AMPK isoforms tested (i.e., α1β2γ3; see Table 1).

To establish whether the stimulation of fat oxidation by the AMPK activator translates into an improvement of NAFLD, we administered compound 1 for 8 weeks to *ob/ob* mice that were pre-fed with the AMLN diet for 12 weeks. Based on the results in KK-A^y mice, we selected an intermediate dose of 5 mg/kg. Over the course of treatment, the AMPK activator neither influenced body weight nor affected food intake in relation to vehicle-treated animals fed the AMLN diet (Fig. 6A,B). The compound reduced liver weight as well as hepatic triglycerides and cholesterol content in relation to the vehicle treatment
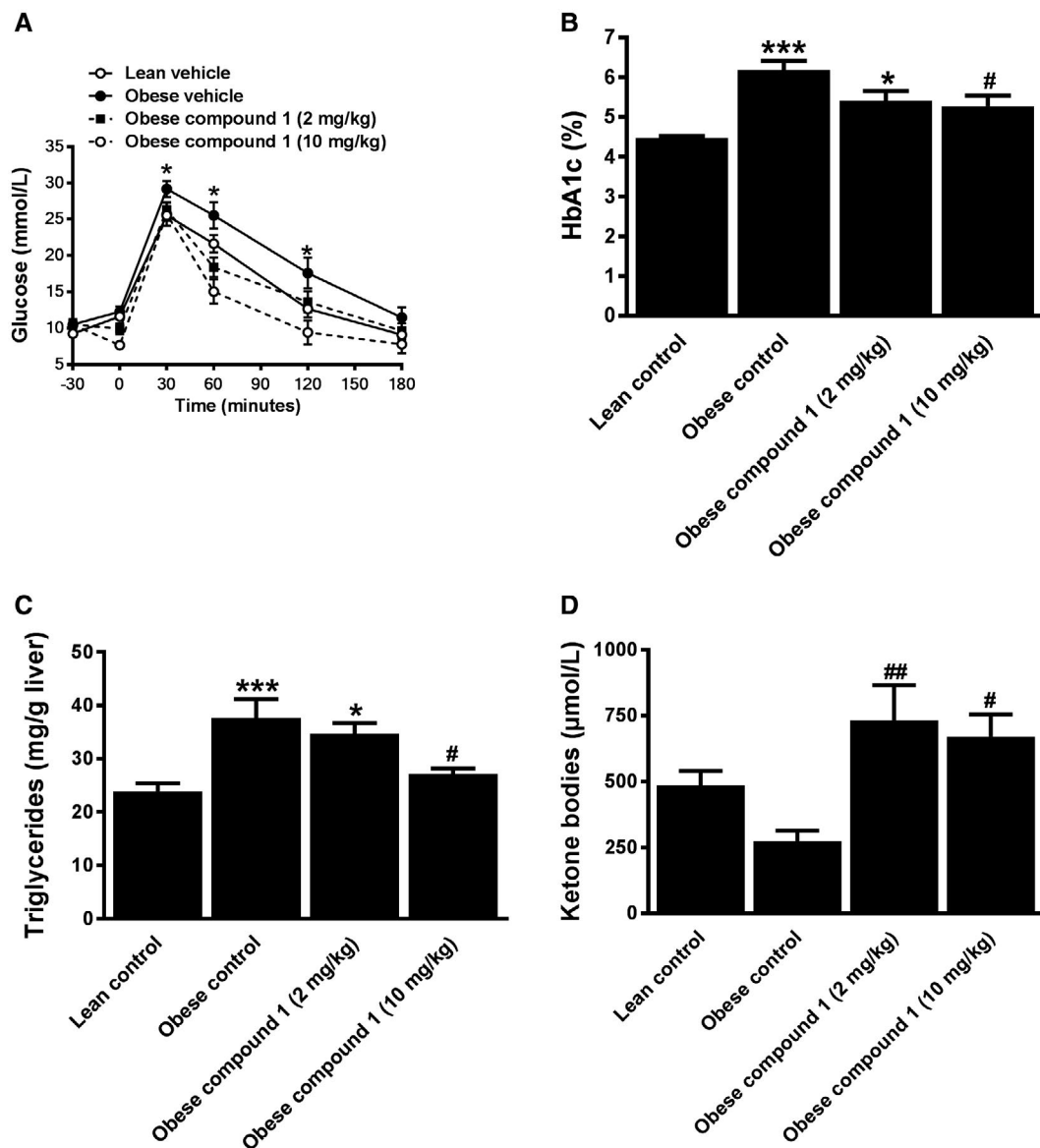
FIG. 4. Acute and chronic effects of compound 1 in KK-A^y mice. (A) Oral glucose tolerance in lean and obese KK-A^y mice. Either vehicle or compound 1 (2 and 10 mg/kg) was administered at $t = -30$ minutes, and glucose bolus (2 g/kg) was given at $t = 0$. Values are presented as means ± SEM (n = 8); *$P < 0.05$ versus lean group. (B) Blood HbA1c, (C) hepatic triglyceride, and (D) serum levels of ketone bodies (β-hydroxybutyrate + acetoacetate) after 3 weeks of treatment with either vehicle or compound 1. Values are presented as means ± SEM; statistical analysis performed with one-way and two-way analysis of variance (ANOVA) with Tukey's multiple comparisons test; *$P < 0.05$ and ***$P < 0.001$ versus the lean control group, and #$P < 0.05$ and ##$P < 0.01$ versus the obese control group (n = 9-10).

(Fig. 6C-E). The activator also lowered plasma liver transaminase activities (Fig. 6H,I), indicating a beneficial effect on liver health. Plasma triglyceride and cholesterol levels were not changed in relation to vehicle-treated animals on the AMLN diet (Fig. 6F,G). Liver biopsies of the animals taken before and after the treatment were histologically examined (Fig. 7).

Seven *ob/ob* mice on standard chow had a steatosis score of 2 and one animal a score of 3, but the animals did not show histological fibrosis, inflammation, or ballooning (data not shown). The *ob/ob* mice fed the AMLN diet for 12 weeks presented fibrosis (Fig. 7A), steatosis (Fig. 7B), and inflammation (Fig. 7D) scores between 1 and 3, and ballooning was detectable in
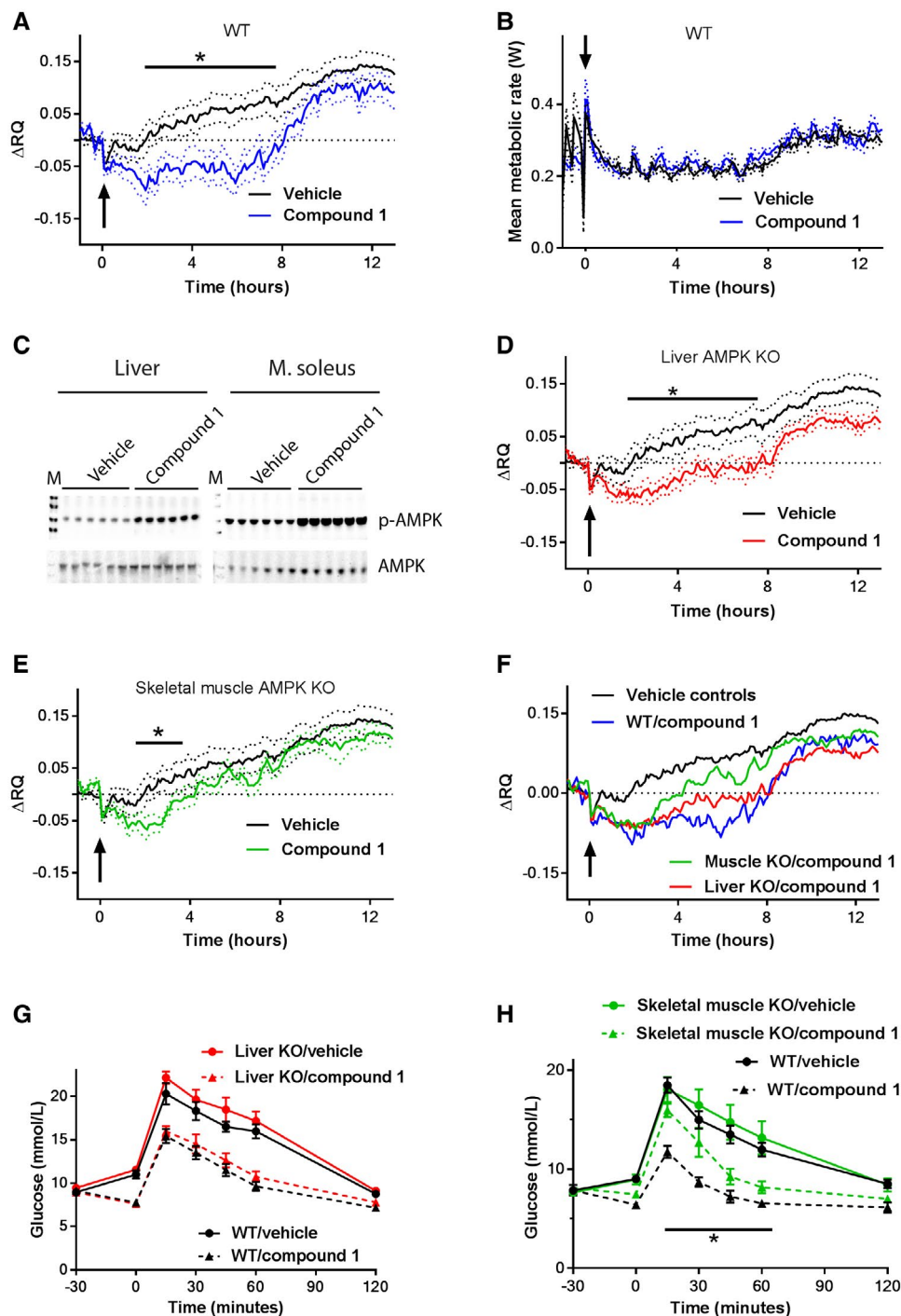
FIG. 5. Indirect calorimetry. (A,B) WT mice (n = 15) or mice lacking AMPK in liver (D) or skeletal muscle (E) were treated with either vehicle or compound 1 (10 mg/kg) at $t = 0$. (A,D-F) ΔRQ versus $t = 0$ was calculated as the ratio of VCO_2 to VO_2. All genotypes of vehicle-treated animals were grouped together. (B) MR of WT animals treated at $t = 0$ with either vehicle or compound 1. (F) Overlay of ΔRQ from (A), (C), and (E). (C) Detection of AMPK activation as determined by increased p-AMPK in liver and soleus muscle by immunoblot analysis. Tissue extracts were prepared 1 hour after the administration of compound 1 (10 mg/kg) or vehicle. Dotted lines indicate respective SEM. Vehicle (combination of all genotypes): n = 22. Treated groups: WT, n = 7; muscle KO, n = 7; liver KO; n = 8. *$P < 0.05$ between vehicle and treatment groups. (G,H) Oral glucose tolerance test in WT mice and mice lacking AMPK either in liver (G) or skeletal muscle (H). Compound 1 was administered at $t = -30$ minutes, and a glucose bolus was given at $t = 0$. Data are presented as means ± SEM (n = 7); *$P < 0.05$ between compound-treated skeletal muscle KO and compound-treated WT mice. Abbreviation: M, molecular weight marker.
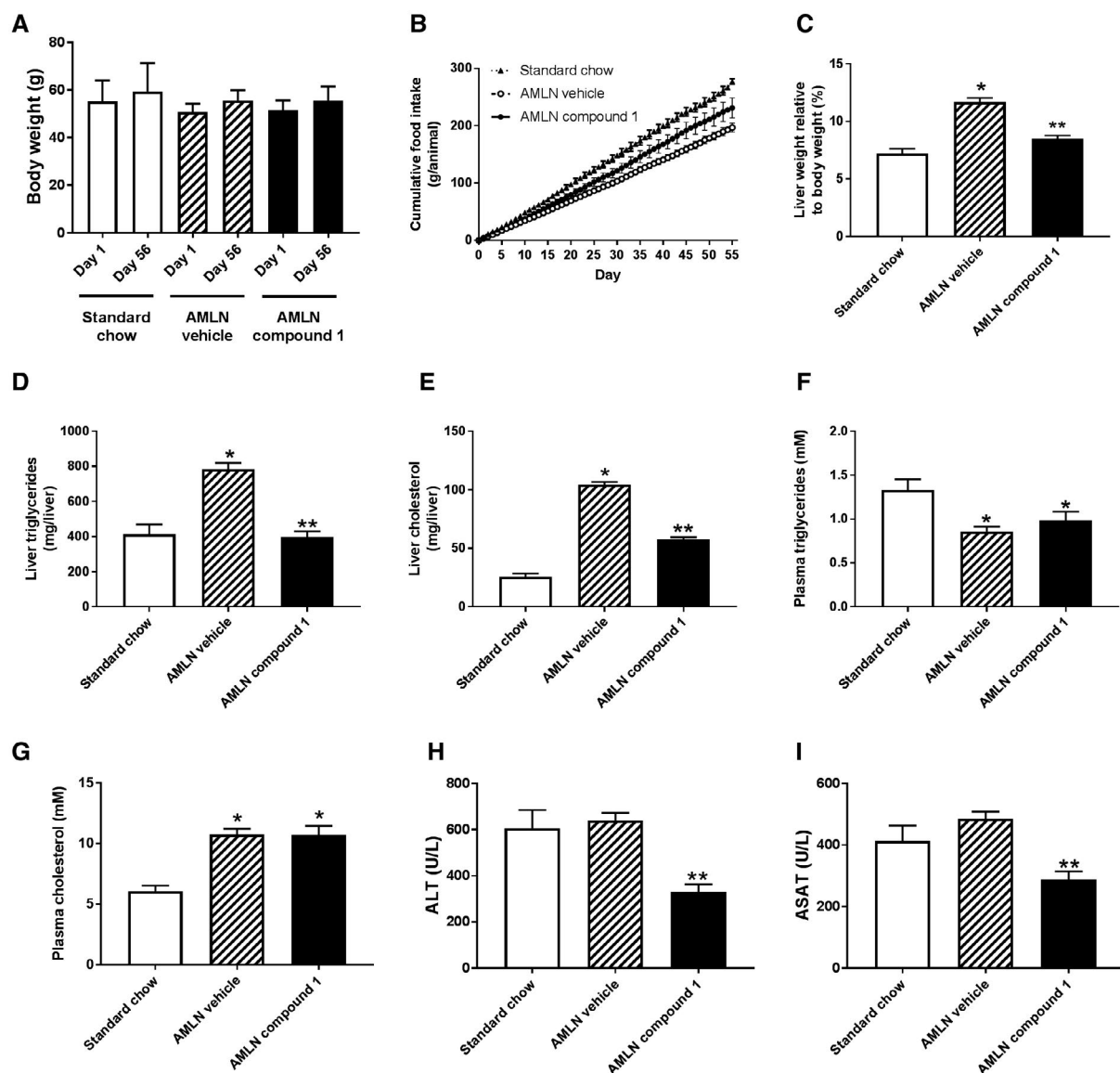
FIG. 6. Characterization of *ob/ob* mice fed either standard chow or AMLN diet. *Ob/ob* mice were pre-fed the AMLN diet for 12 weeks, followed by the daily administration of either compound 1 (3 mg/kg) or vehicle for 8 weeks. Body-weight development (A) and food intake (B) during treatment period. Liver weight (C), liver triglyceride (D), liver cholesterol (E), plasma triglyceride (F), plasma cholesterol (G), and the plasma transaminases alanine aminotransferase (H) and aspartate aminotransferase (I) were determined at the end of the treatment. *$P < 0.001$ versus animals on standard chow; **$P < 0.001$ versus vehicle-treated AMLN animals (data are presented as means ± SEM; n = 8-9); one-way ANOVA with Dunnett's multiple comparison test. Abbreviations: ALT, alanine aminotransferase; ASAT, aspartate aminotransferase.

four animals (Fig. 7C). Posttreatment biopsies showed a significant inhibition of fibrosis progression by compound 1 (Fig. 7A). Improvements of ballooning and steatosis were close to significance (Fig. 7B,C). The treatment with the AMPK activator did not show effectiveness on the inflammation score in relation to vehicle treatment (Fig. 7D). Compound 1 significantly

ameliorated worsening of the NAFLD activity score (Fig. 7E). In line with an increased fibrosis score, the AMLN diet elevated hepatic expression of the profibrotic gene *Col1a1* (Fig. 8). The administration of the AMPK activator attenuated this induction. Overall, these data demonstrate that the AMPK activator has a beneficial effect on liver health in the NASH
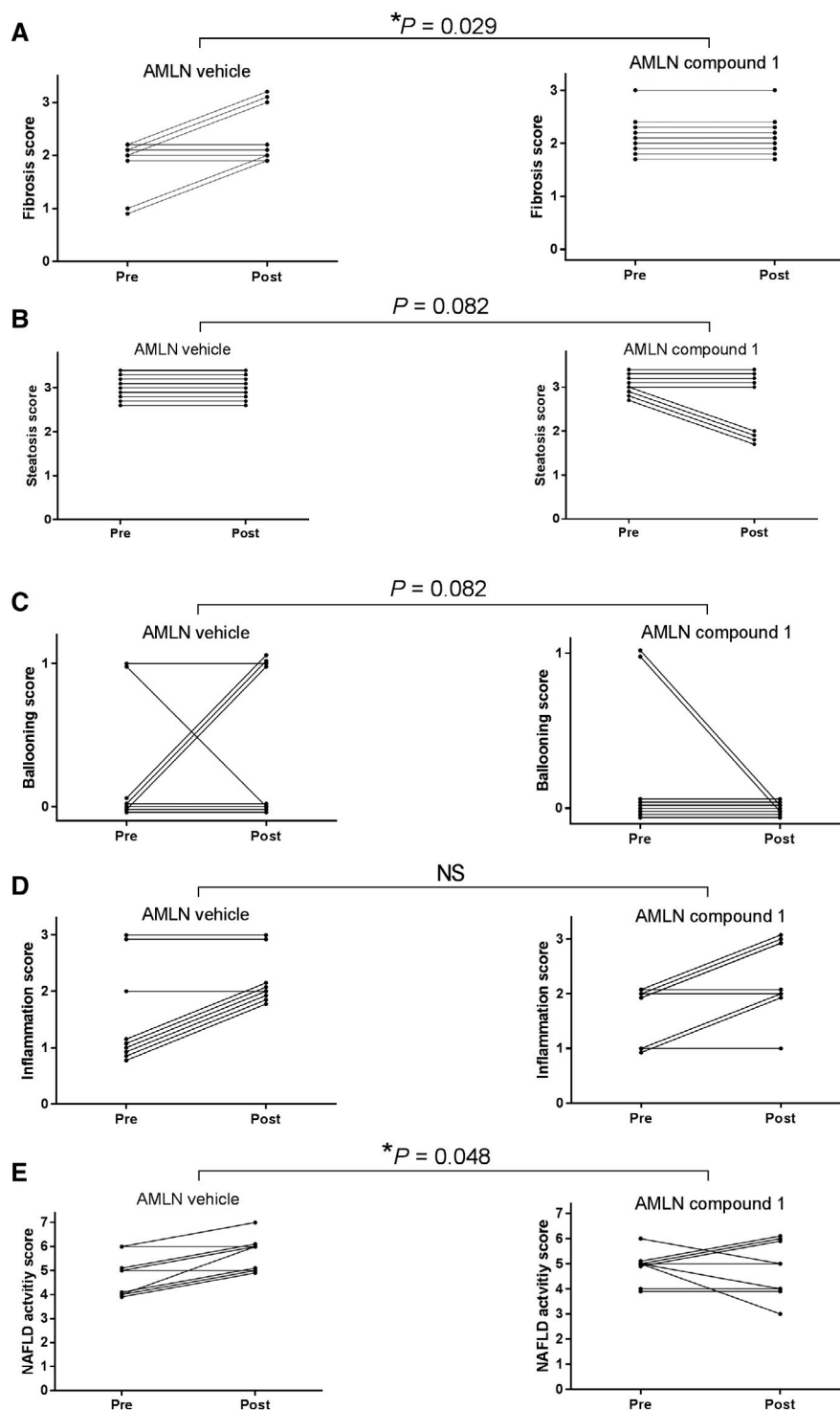
FIG. 7. Histological assessment of NAFLD progression. Histological assessment of each *ob/ob* mouse fed the AMLN diet based on liver biopsies before (pre) and at the end (post) of the treatment with either vehicle or compound 1 (3 mg/kg). Animals were fed the AMLN diet for 12 weeks and subsequently the diet together with either vehicle or compound 1: fibrosis score (A), steatosis score (B), ballooning score (C), inflammation score (D), and NAFLD activity score (E). The points at each scoring step are slightly shifted to allow visual separation of the animals (this is only for visualization purposes and does not reflect any differences in score). Indicated are significances for differences in progression of pre or post scores in case of equal pre values of the respective parameters between vehicle-treated and compound-treated groups calculated using Fisher's exact test (A-D) for two levels and Wilcoxon exact test (E) for more than two levels.
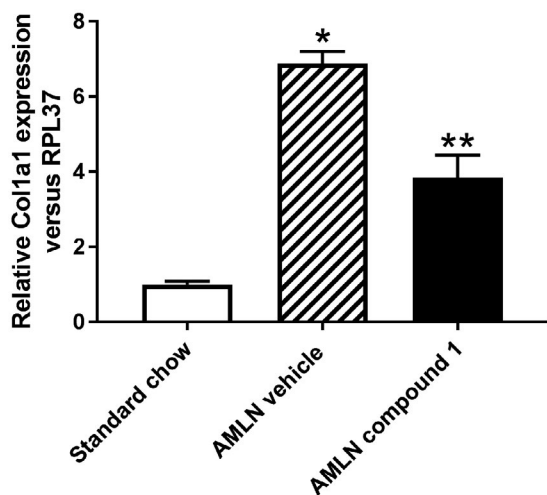
FIG. 8. Regulation of hepatic expression of Col1a1. *ob/ob* mice were fed either standard chow or the AMLN diet. The latter were treated with either vehicle or compound 1 for 8 weeks. RNA was isolated from liver. RNA levels of Col1a1 in relation to RPL37a were determined by quantitative RT-PCR, and controls (standard chow) were set as 1. The data are presented as means ± SEM (n = 8-9); *$P < 0.05$ versus control, and **$P < 0.05$ versus control and vehicle-treated animals; one-way ANOVA.

model, predominately by improving hepatic steatosis and reducing the progression of liver fibrosis.

Because NASH predisposes to the development of liver cancer, we tested the effect of the compound on the development of diet-induced HCC. C57BL/6J mice were fed for 68 weeks with the AMLN diet, followed by the administration of either vehicle or compound 1 (3 mg/kg) for 12 weeks. Compound 1 did not affect body weight gain (Fig. 9A) but reduced liver weight (Fig. 9B) and decreased hepatic triglycerides as well as cholesterol content, indicating an antisteatotic effect (Fig. 9C,D). Plasma liver transaminase levels were also decreased by the AMPK activator (Fig. 9E,F). Histological examination of biopsies taken before the onset of treatment demonstrated that feeding the animals for the prolonged period of time led to more advanced hepatic fibrosis, ballooning, and inflammation than observed in the *ob/ob* animals that were pre-fed for 12 weeks (Fig. 7 vs. Fig. 9). In relation to vehicle treatment, the administration of compound 1 did not significantly improve fibrosis, ballooning, or inflammation (Fig. 10A,C,D). Histological steatosis and the deterioration of the NAFLD activity score were improved close to significance (Fig. 10B,E). In animals fed the AMLN diet over 80 weeks, HCCs

were detectable (Fig. 11A). The administration of the AMPK activator significantly reduced the tumor incidence as well as size (Fig. 11B-D). Gene-expression analysis of whole-liver homogenates revealed the induction of the HCC markers *SDK1, UBD,* and *LCN2* in vehicle-treated animals fed the AMLN diet in relation to animals fed the standard chow (Fig. 12A). The administration of compound 1 reduced the expression of these genes. Immunoblots of whole-liver extracts revealed a down-regulation of the UBD-target protein WISP1 in response to the AMLN diet, which was, however, not significantly reversed by compound 1 (Fig. 12B).

Discussion

Genetic[10-13] and pharmacological[7] activation of AMPK in liver improves hepatic steatosis. This led to the hypothesis that AMPK activation could be useful for the treatment of early stages of NAFLD. The present paper confirms and extends these observations. Our experimental design differs from previous reports by the use of a dedicated murine model of advanced NASH with fibrosis and by the pharmacological activation of AMPK not only in liver but also in muscle.

Compound 1 activates AMPK in muscle due to its PK profile and its ability to activate all isoforms of AMPK, including those containing the β2 subunits that are predominantly expressed in muscle. The glucose-lowering effect of AMPK activation is caused primarily by the stimulation of AMPK in muscle.[6,8] We confirmed these data and thereby validated our genetic models by the demonstration that the loss of AMPK in skeletal muscle, but not in liver, attenuated the beneficial effect of the compound on glucose tolerance. Genetic models have provided contradictory results concerning whether the stimulation of AMPK affects whole-body fat oxidation,[11-13] and pharmacological studies with selective activators have not yet been carried out. As shown here, AMPK activation by compound 1 lowered the RQ and stimulated fat oxidation *in vivo*. The data obtained by studying muscle-selective and liver-selective AMPK knockout (KO) indicate that the activation of AMPK in skeletal muscle by compound 1 is not only important for improved glucose tolerance but also has a major contribution to the stimulation of whole-body fat oxidation. Increased
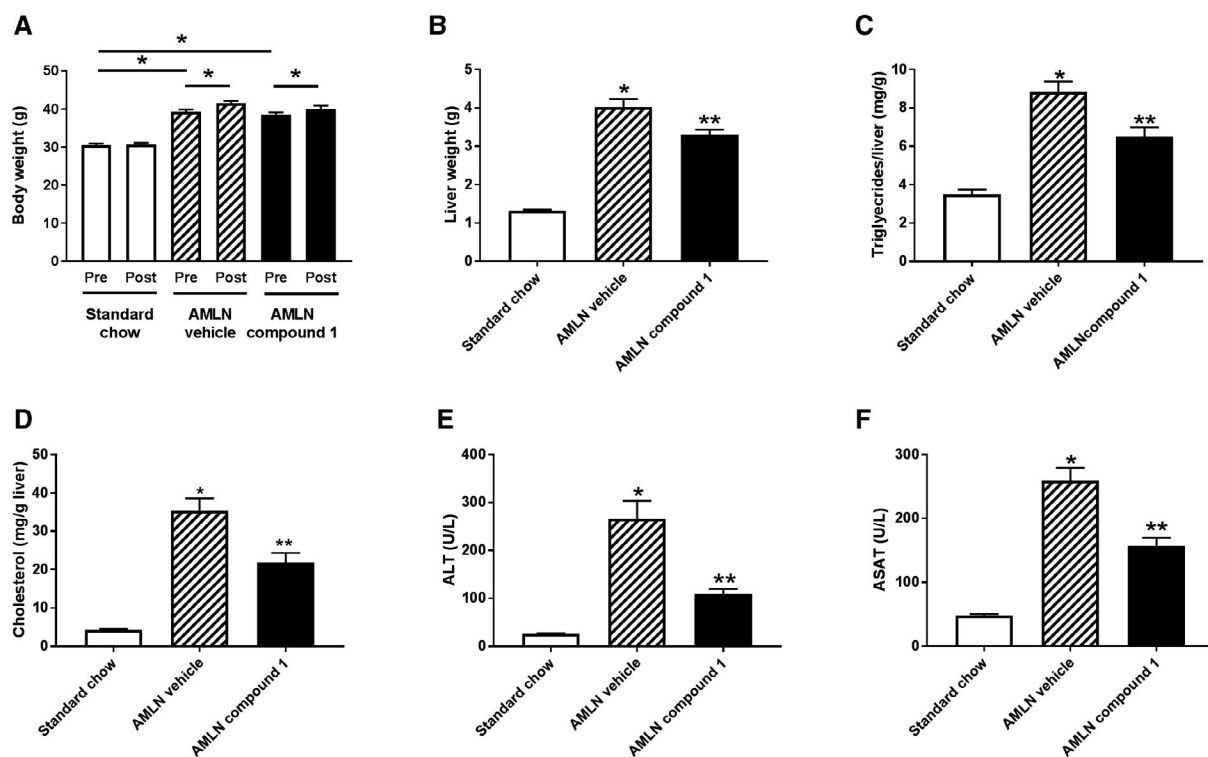
FIG. 9. Terminal characterization of mice after 80 weeks on AMLN diet. Mice were fed either standard chow or AMLN diet for 68 weeks, followed by the administration of either vehicle or compound 1 (5 mg/kg) as indicated for 12 weeks. (A) Body weights before (pre) and after (post) onset of the administration of either vehicle or compound 1: liver weight (B), hepatic triglyceride (C), and cholesterol content (D). (E,F) Plasma transaminase levels at the end of the treatment. The data are presented as means ± SEM (n = 10-16); $^*P < 0.05$ versus control, and $^{**}P < 0.05$ versus control-treated and vehicle-treated animals; Dunnett's test one-factor linear model. Abbreviations: ALT, alanine aminotransferase; ASAT, aspartate aminotransferase.

fat oxidation is crucial for the reduced hepatic steatosis on AMPK activation in the animals fed the high-fat diet.[10,11] At the same time, steatosis is closely linked to NAFLD progression.[3,25] Compound 1 shows efficacy on hepatic lipids at much lower doses than PF-06409577.[7] This cannot be explained by the PK profiles of these compounds, but is due to the failure of PF-06409577 to activate AMPK in muscle caused by its selectivity toward β1-containing AMPK trimers.[9] We postulate that the ability of compound 1 to target muscle is not only essential for its antidiabetic effect, but also increases its potency on improving hepatic steatosis and NAFLD progression.

Genetic models provided conflicting results regarding the reduction in body weight by hepatic AMPK activation.[12,13] In our study, compound 1 did not change the body weight, even after administration for up to 12 weeks. This is supported by the observation that compound 1 altered neither MR nor food intake. The improvement of steatosis by compound 1 in the NAFLD models was therefore not secondary to weight loss but was caused by metabolic changes such as fuel switching, which was demonstrated by our indirect calorimetry data.

We initially studied the efficacy of compound 1 on NAFLD in *ob/ob* mice fed with the AMLN diet for 20 weeks. In contrast to animals fed a high-fat diet, as used before to characterize the effect of pharmacological or genetic AMPK activation on NAFLD,[7,12] these mice develop histological features of NASH, including fibrosis, with only a moderate increase of body weight.[18,19] The animals were biopsied before and after the treatment. This allowed randomization of the animals according to the extent of fibrosis and the histological evaluation of treatment efficacy for each animal individually. Not only plasma liver transaminase levels but also worsening of the fibrosis score was significantly
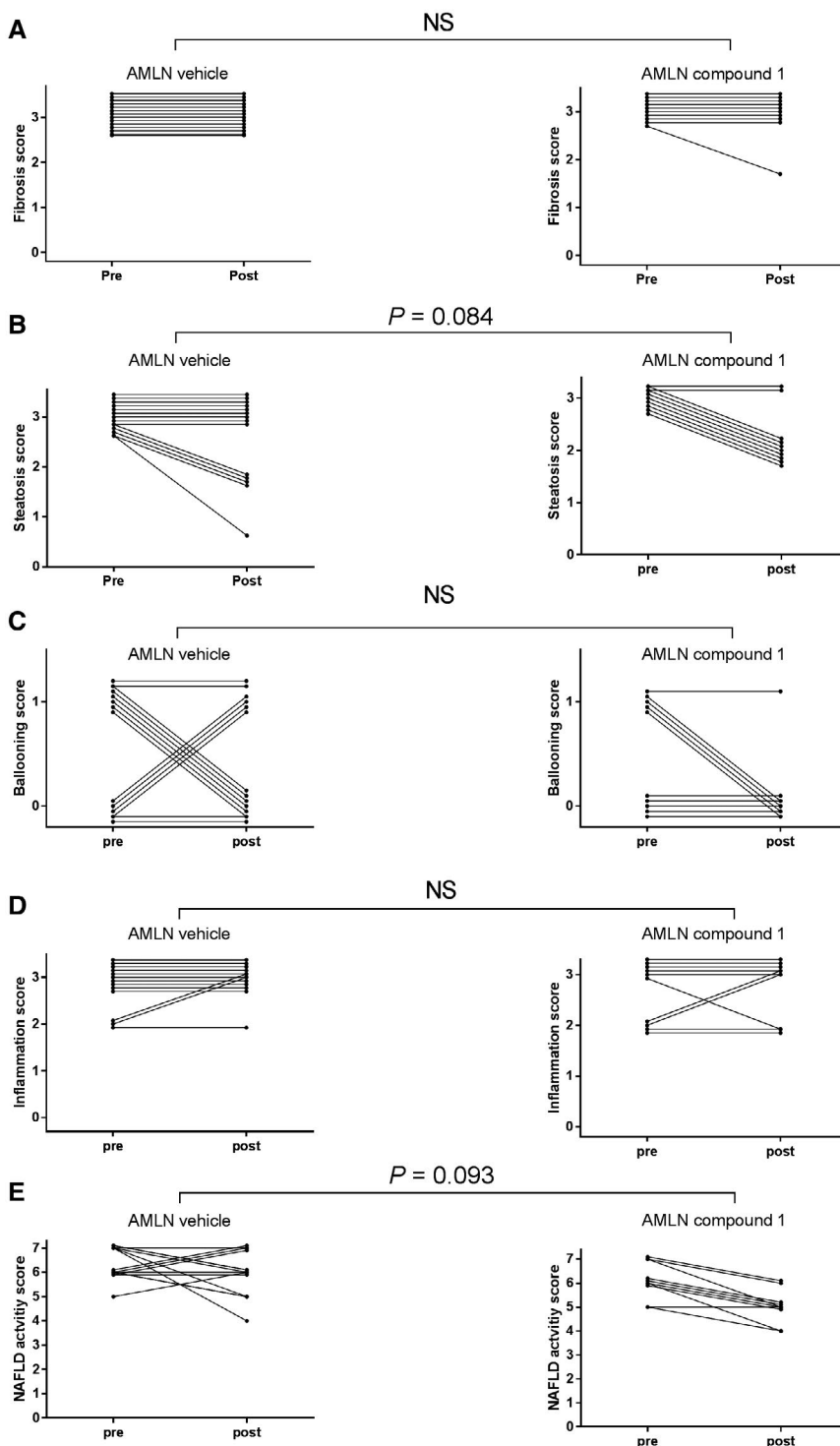
FIG. 10. Histological assessment of NAFLD progression. Histological assessment of each mouse fed the AMLN diet before (pre) and at the end (post) of the treatment with either vehicle or compound 1 (5 mg/kg). Animals were initially fed for 68 weeks, biopsied, and then subsequently fed the AMLN diet for 12 additional weeks in the presence of either vehicle or compound 1: fibrosis score (A), steatosis score (B), ballooning score (C), inflammation score (D), and NAFLD activity score (E). The points at each scoring step are slightly shifted to allow visual separation of the animals (this is only for visualization purposes and does not reflect any differences in score). Indicated are significances for differences in progression of the respective parameters between vehicle-treated and compound-treated groups calculated using Fisher's exact test for two levels (A) and Wilcoxon exact test for more than two levels (B-E). Abbreviation: NS, not significant.
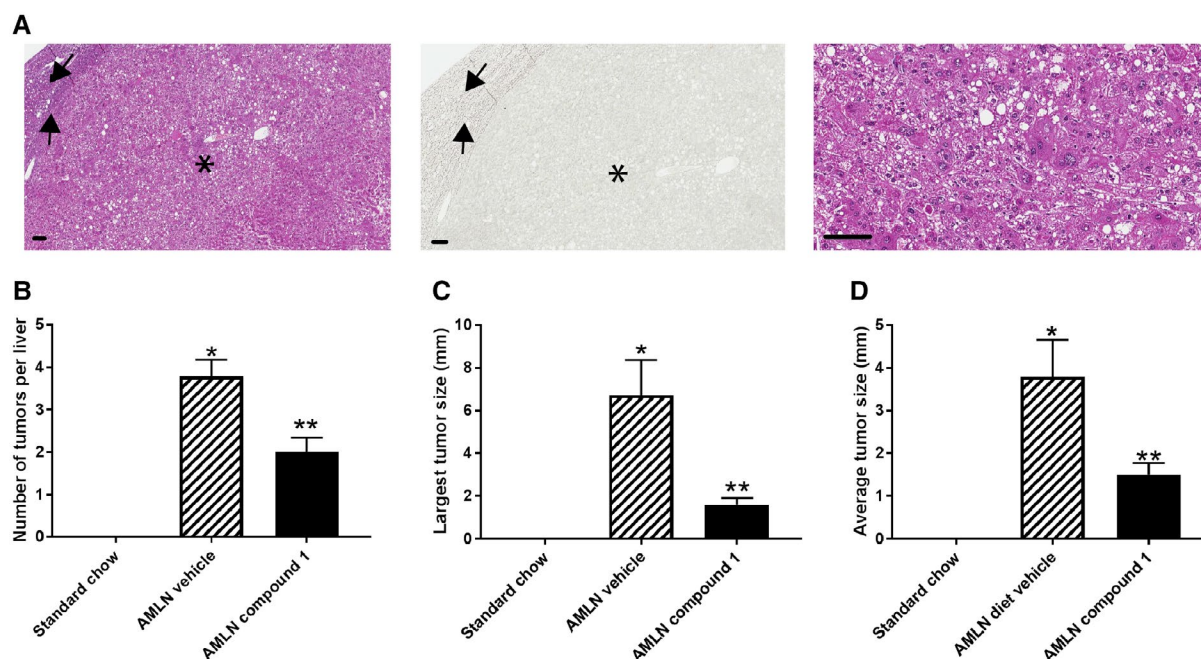
FIG. 11. Tumor assessment in mice fed the AMLN diet for 80 weeks. (A) HE-stained liver sections (left and right panels at different magnification) and reticulin-stained liver sections (middle panel) from a vehicle animal fed the AMLN diet for 80 weeks and showing a HCC with loss of the normal lobuloalveolar architecture (asterisk marks a large carcinoma, and arrows indicate liver parenchyma with a compression zone in between the two). The image of high magnification shows cellular and nuclear pleomorphism. Scale bars represent 100 μm. (B-D) Histological assessment of livers with respect to number of tumors (B), largest tumor size (C), and average tumor size (D). The data are presented as means ± SEM (n = 10-16); *$P < 0.001$ versus control, and **$P < 0.001$ versus control-treated and vehicle-treated animals; Dunnett's test one-factor linear model.

improved by compound 1. This was paralleled by decreased hepatic expression of the profibrotic gene *Col1a1*. These data demonstrate that the pharmacological activation of AMPK has beneficial effects on liver health in addition to improving steatosis. Genetic AMPK activation in heart protects against fibrosis by reducing transforming growth factor β signaling.[26] A similar mechanism might be responsible for the antifibrotic effect of compound 1 in the NAFLD model. Furthermore, AMPK activation has been shown to inhibit the proliferation and activation of hepatic stellate cells, the principal hepatic cell type responsible for liver fibrosis.[27,28] Although genetic models and unselective AMPK activators suggest an anti-inflammatory action of AMPK activation,[29] compound 1 did not significantly improve histological inflammation in our disease model.

Mice fed the AMLN diet for 68 weeks had advanced liver damage, as indicated by a high fibrosis score. Subsequent administration of compound 1 failed to improve this parameter. Thus, the beneficial

effect of AMPK activation appears to affect predominantly fibrosis progression but not resolution. The prolonged feeding with the AMLN diet resulted in the onset of HCC. This was reflected by both an altered histology and the increased expression of *UBD*, *SDK1*, and *LCN2*, which are genetic markers for HCC.[30-33] Notably, compound 1 reduced tumor incidence and size when administered over the last 12 weeks of diet. This provides preclinical evidence that a selective AMPK activator can ameliorate the progression of NAFLD to HCC. Our results are supported by initial genetic evidence that AMPK could act as a tumor suppressor[34] and epidemiological data indicating a potential anticancer activity of the unselective AMPK activator metformin.[35,36]

Multiple, mutually nonexclusive mechanisms by which AMPK might prevent tumor growth have been described.[25,37-40] A mutation of the inhibitory AMPK-phosphorylation site within ACC promotes hepatic steatosis and fibrosis in mice[41] and increases liver lesions in a model of chemical-induced
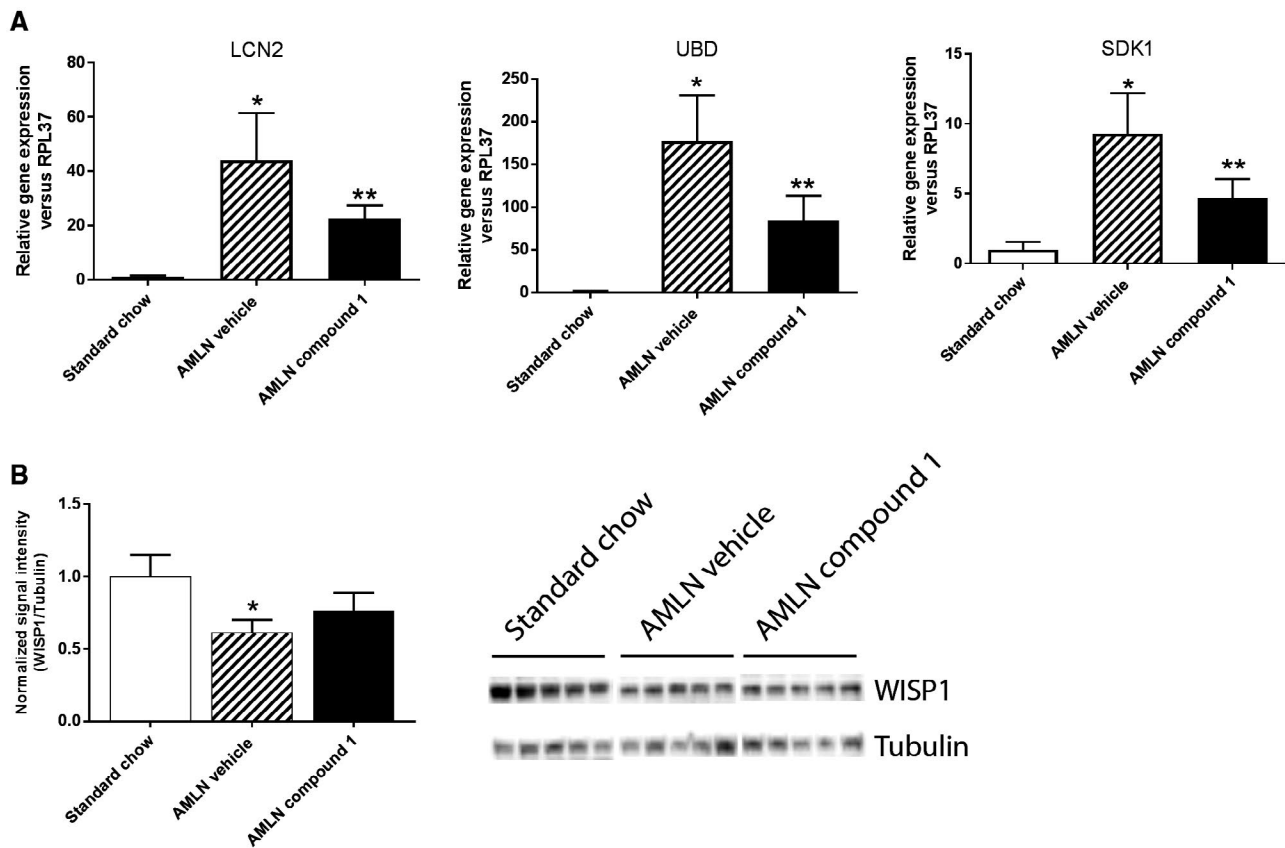
FIG. 12. Regulation of hepatic expression of HCC markers. Mice were fed either standard chow or the AMLN diet for 68 weeks before being administered either vehicle or compound 1 for 12 weeks. (A) RNA was isolated from whole-liver tissue of mice treated as indicated. Messenger RNA levels of UBD, SDK1, LCN2, and RPL37 were determined by quantitative RT-PCR, and controls (standard chow) were set as 1. (B) Whole-liver lysates were electrophoresed by sodium dodecyl sulfate–polyacrylamide gel electrophoresis and transferred onto nylon membranes. Western blots, as exemplified in the right panel, were performed using antibodies against WISP1 and tubulin as loading control. The data are presented as means ± SEM (n = 10-16); *$P < 0.05$ versus standard chow, and **$P < 0.05$ versus control-treated and vehicle-treated animals; t test.

hepatocarcinogenesis, whereas the direct inhibition of ACC had a beneficial effect.[40] ACC is central for the control of fat oxidation and *de novo* lipogenesis, and the data concluded that an antisteatotic effect is beneficial for the suppression of liver lesions in this model.[40] Compound 1 had an antisteatotic effect; therefore, this mechanism might also contribute to the decreased HCC incidence in a model of diet-induced HCC. Compound 1 also partially reversed the up-regulation of *SDK1, LCN2,* and *UBD* expression in the disease model. The mechanism by which AMPK activation regulates these genes is unknown. Increased expression of *LCN2* is regarded as a biomarker of HCC, and it is unclear whether it promotes carcinogenesis.[33] However, *SDK1,* an epigenetically

regulated gene that encodes for a cell-adhesion protein, is frequently mutated in both murine and human NASH and is considered a driver of cancer pathogenesis by unknown mechanisms.[31,32] Likewise, the up-regulation of the ubiquitin-like modifier UBD contributes to the progression and severity of HCC.[42] Among the discussed mechanisms is the subsequent degradation of WISP1 and modification of Wnt signaling.[43] We noticed decreased protein levels of WISP1 in the liver of AMLN-fed animals but did not detect a significant up-regulation of the protein in response to our AMPK activator. This could be due to the high variability of the biological material, because we worked with whole-liver homogenates. Overall, we speculate that, in addition to an antisteatotic effect,

the modulation of SDK1 and UBD could be among the mechanisms by which AMPK activation reduced tumor incidence in the animal model of diet-induced HCC.

In conclusion, our data qualify pharmacological AMPK activation in liver and skeletal muscle as a potential approach to prevent the progression of NAFLD to HCC. Future studies with isoform-selective and tissue-selective AMPK activators are required to identify the optimal profile of a small-molecule drug to exhibit beneficial effects on NAFLD without having potential side effects, such as heart toxicity.[6]

REFERENCES

1) Anstee QM, Reeves HL, Kotsiliti E, Govaere O, Heikenwalder M. From NASH to HCC: current concepts and future challenges. Nat Rev Gastroenterol Hepatol 2019;16:411-428.

2) Olofson AM, Gonzalo DH, Chang M, Liu X. Steatohepatitic variant of hepatocellular carcinoma: a focused review. Gastroenterology Res 2018;11:391-396.

3) Schuster S, Cabrera D, Arrese M, Feldstein AE. Triggering and resolution of inflammation in NASH. Nat Rev Gastroenterol Hepatol 2018;15:349-364.

4) Steinberg GR, Carling D. AMP-activated protein kinase: the current landscape for drug development. Nat Rev Drug Discov 2019;18:527-551.

5) Lin SC, Hardie DG. AMPK: sensing glucose as well as cellular energy status. Cell Metab 2018;27:299-313.

6) Myers RW, Guan HP, Ehrhart J, Petrov A, Prahalada S, Tozzo E, et al. Systemic pan-AMPK activator MK-8722 improves glucose homeostasis but induces cardiac hypertrophy. Science 2017;357:507-511.

7) Esquejo RM, Salatto CT, Delmore J, Albuquerque B, Reyes A, Shi Y, et al. Activation of liver AMPK with PF-06409577 corrects NAFLD and lowers cholesterol in rodent and primate preclinical models. EBioMedicine 2018;31:122-132.

8) Cokorinos EC, Delmore J, Reyes AR, Albuquerque B, Kjobsted R, Jorgensen NO, et al. Activation of skeletal muscle AMPK promotes glucose disposal and glucose lowering in non-human primates and mice. Cell Metab 2017;25:1147-1159.e1110.

9) Salatto CT, Miller RA, Cameron KO, Cokorinos E, Reyes A, Ward J, et al. Selective activation of AMPK beta1-containing isoforms improves kidney function in a rat model of diabetic nephropathy. J Pharmacol Exp Ther 2017;361:303-311.

10) Boudaba N, Marion A, Huet C, Pierre R, Viollet B, Foretz M. AMPK re-activation suppresses hepatic steatosis but its downregulation does not promote fatty liver development. EBioMedicine 2018;28:194-209.

11) Foretz M, Even PC, Viollet B. AMPK activation reduces hepatic lipid content by increasing fat oxidation in vivo. Int J Mol Sci 2018;19:2826.

12) Garcia D, Hellberg K, Chaix A, Wallace M, Herzig S, Badur MG, et al. Genetic liver-specific AMPK activation protects against diet-induced obesity and NAFLD. Cell Rep 2019;26:192-208.e196.

13) Woods A, Williams JR, Muckett PJ, Mayer FV, Liljevald M, Bohlooly YM, et al. Liver-specific activation of AMPK prevents steatosis on a high-fructose diet. Cell Rep 2017;18:3043-3051.

14) Tamura YH, Hinata Y, Kojima E, Ozasa H, inventors; Shionogi & Co., Ltd., assignee. Azaindole derivative having AMPK-activating effect. US patent number WO2016/031842A1. March 3, 2016.

15) Keil S, Müller M, Zoller G, Haschke G, Schroeter K, Glien M, et al. Identification and synthesis of novel inhibitors of acetyl-CoA carboxylase with in vitro and in vivo efficacy on fat oxidation. J Med Chem 2010;53:8679-8687.

16) Schummer CM, Werner U, Tennagels N, Schmoll D, Haschke G, Juretschke HP, et al. Dysregulated pyruvate dehydrogenase complex in Zucker diabetic fatty rats. Am J Physiol Endocrinol Metab 2008;294:E88-E96.

17) Glien M, Haschke G, Schroeter K, Pfenninger A, Zoller G, Keil S, et al. Stimulation of fat oxidation, but no sustained reduction of hepatic lipids by prolonged pharmacological inhibition of acetyl CoA carboxylase. Horm Metab Res 2011;43:601-606.

18) Kristiansen MN, Veidal SS, Rigbolt KT, Tolbol KS, Roth JD, Jelsing J, et al. Obese diet-induced mouse models of nonalcoholic steatohepatitis-tracking disease by liver biopsy. World J Hepatol 2016;8:673-684.

19) Roth JD, Feigh M, Veidal SS, Fensholdt LK, Rigbolt KT, Hansen HH, et al. INT-767 improves histopathological features in a diet-induced ob/ob mouse model of biopsy-confirmed nonalcoholic steatohepatitis. World J Gastroenterol 2018;24:195-210.

20) Kleiner DE, Brunt EM, Van Natta M, Behling C, Contos MJ, Cummings OW, et al. Design and validation of a histological scoring system for nonalcoholic fatty liver disease. Hepatology 2005;41:1313-1321.

21) Lantier L, Fentz J, Mounier R, Leclerc J, Treebak JT, Pehmoller C, et al. AMPK controls exercise endurance, mitochondrial oxidative capacity, and skeletal muscle integrity. FASEB J 2014;28:3211-3224.

22) Even PC, Nadkarni NA. Indirect calorimetry in laboratory mice and rats: principles, practical considerations, interpretation and perspectives. Am J Physiol Regul Integr Comp Physiol 2012;303:R459-R476.

23) Weir JB. New methods for calculating metabolic rate with special reference to protein metabolism. J Physiol 1949;109:1-9.

24) Winkel AF, Engel CK, Margerie D, Kannt A, Szillat H, Glombik H, et al. Characterization of RA839, a noncovalent small molecule binder to Keap1 and selective activator of Nrf2 signaling. J Biol Chem 2015;290:28446-28455.

25) Hirsova P, Ibrahim SH, Gores GJ, Malhi H. Lipotoxic lethal and sublethal stress signaling in hepatocytes: relevance to NASH pathogenesis. J Lipid Res 2016;57:1758-1770.

26) Hinson JT, Chopra A, Lowe A, Sheng CC, Gupta RM, Kuppusamy R, et al. Integrative analysis of PRKAG2 cardiomyopathy iPS and microtissue models identifies AMPK as a regulator of metabolism, survival, and fibrosis. Cell Rep 2016;17:3292-3304.

27) Adachi M, Brenner DA. High molecular weight adiponectin inhibits proliferation of hepatic stellate cells via activation of adenosine monophosphate-activated protein kinase. Hepatology 2008;47:677-685.

28) Caligiuri A, Bertolani C, Guerra CT, Aleffi S, Galastri S, Trappoliere M, et al. Adenosine monophosphate-activated protein kinase modulates the activated phenotype of hepatic stellate cells. Hepatology 2008;47:668-676.

29) Day EA, Ford RJ, Steinberg GR. AMPK as a therapeutic target for treating metabolic diseases. Trends Endocrinol Metab 2017;28:545-560.

30) Aichem A, Groettrup M. The ubiquitin-like modifier FAT10 in cancer development. Int J Biochem Cell Biol 2016;79:451-461.

31) Gentilini D, Scala S, Gaudenzi G, Garagnani P, Capri M, Cescon M, et al. Epigenome-wide association study in hepatocellular carcinoma: identification of stochastic epigenetic mutations through an innovative statistical approach. Oncotarget 2017;8:41890-41902.

32) Liang JQ, Teoh N, Xu L, Pok S, Li X, Chu ESH, et al. Dietary cholesterol promotes steatohepatitis related hepatocellular carcinoma through dysregulated metabolism and calcium signaling. Nat Commun 2018;9:4490.

33) Asimakopoulou A, Vucur M, Luedde T, Schneiders S, Kalampoka S, Weiss TS, et al. Perilipin 5 and lipocalin 2 expression in hepatocellular carcinoma. Cancers (Basel) 2019;11:385.

34) Vara-Ciruelos D, Russell FM, Hardie DG. The strange case of AMPK and cancer: Dr Jekyll or Mr Hyde? Open Biol 2019;9:190099.

35) Vancura A, Bu P, Bhagwat M, Zeng J, Vancurova I. Metformin as an anticancer agent. Trends Pharmacol Sci 2018;39:867-878.

36) Iranshahy M, Rezaee R, Karimi G. Hepatoprotective activity of metformin: a new mission for an old drug? Eur J Pharmacol 2019;850:1-7.

37) Wu D, Hu D, Chen H, Shi G, Fetahu IS, Wu F, et al. Glucose-regulated phosphorylation of TET2 by AMPK reveals a pathway linking diabetes to cancer. Nature 2018;559:637-641.

38) Troncone M, Cargnelli SM, Villani LA, Isfahanian N, Broadfield LA, Zychla L, et al. Targeting metabolism and AMP-activated kinase with metformin to sensitize non-small cell lung cancer (NSCLC) to cytotoxic therapy: translational biology and rationale for current clinical trials. Oncotarget 2017;8:57733-57754.

39) Lee SB, Kim JJ, Han SA, Fan Y, Guo LS, Aziz K, et al. The AMPK-Parkin axis negatively regulates necroptosis and tumorigenesis by inhibiting the necrosome. Nat Cell Biol 2019;21:940-951.

40) Lally JSV, Ghoshal S, DePeralta DK, Moaven O, Wei L, Masia R, et al. Inhibition of acetyl-CoA carboxylase by phosphorylation or the inhibitor ND-654 suppresses lipogenesis and hepatocellular carcinoma. Cell Metab 2019;29:174-182.e175.

41) Fullerton MD, Galic S, Marcinko K, Sikkema S, Pulinilkunnil T, Chen ZP, et al. Single phosphorylation sites in Acc1 and Acc2 regulate lipid homeostasis and the insulin-sensitizing effects of metformin. Nat Med 2013;19:1649-1654.

42) Yuan R, Wang K, Hu J, Yan C, Li M, Yu X, et al. Ubiquitin-like protein FAT10 promotes the invasion and metastasis of hepatocellular carcinoma by modifying beta-catenin degradation. Cancer Res 2014;74:5287-5300.

43) Yan J, Lei J, Chen L, Deng H, Dong D, Jin T, et al. Human leukocyte antigen F locus adjacent transcript 10 overexpression disturbs WISP1 protein and mRNA expression to promote hepatocellular carcinoma progression. Hepatology 2018;68:2268-2284.

Supporting Information